A long non-coding RNA, *afu-254*, is required for the oxidative stress response, cell wall stress response, azole susceptibility and virulence in *Aspergillus fumigatus*

Ritu Devkota[1,2,*], Nava Poudyal[1,2], Jazmin Reyes Servin[3], Julianna Lenz[3], Kelly M. Shepardson[3], and Sourabh Dhingra[1,2,4]

1. Department of Biological Sciences, Clemson University, Clemson, SC, 29634
2. Eukaryotic Pathogen Innovation Center, Clemson University, Clemson, SC, 29634
3. Molecular Cell Biology Department, University of California Merced, Merced, CA, 95343
4. Address correspondence to: sdhingr@clemson.edu

[*] Current affiliation – Research Associate, SystImmune, ritu.devkota15@gmail.com

Abstract:

Long non-coding RNAs play an important role in stress response in all forms of life; however, a tight regulation of lncRNAs is required for normal function. Abnormal expression of lncRNA is associated with uncontrolled cell growth in many forms of cancer. Recent studies have highlighted the role of lncRNAs in *Aspergillus fumigatus* in azole stress response and virulence. Here, using a transcriptome dataset of *A. fumigatus* response to stress, we identified *afu-254* as an 854bp lncRNA that plays a role in modulating oxidative stress, fungal ARC response, cell wall stress, macrophage phagocytosis and killing *ex vivo*, and virulence in an invertebrate model of *Aspergillus* infection. Importantly, *afu-254* does not produce cross-azole susceptible response and plays a role in fungal azole response against posaconazole and itraconazole but not voriconazole. Furthermore, we showed that stochiometric levels of *afu-254* are important for its function, and ectopic overexpression of *afu-254* in the WT strain leads to an antimorph. This phenotype is due to a higher ordered structure that is denatured with heat, indicating the presence of a non-functional structure. In conclusion, we characterized a novel lncRNA, *afu-254*, that is important for stress response and virulence in the pathogenic fungus *A. fumigatus*.

31 **Importance:**

32 Failure of azole treatment for invasive *Aspergillus* infection by both drug-resistant and drug-
33 sensitive isolates is an area of concern and global importance. Fungal stress response is
34 multifaceted, and long non-coding RNAs have emerged as important players in mediating
35 it, including regulating responses to azole antifungals. Here, we have identified a long non-
36 coding RNA, *afu-254*, that plays a role in modulating fungal response to oxidative stress,
37 cell wall stress, azole stress, immune cell stress and is indispensable for virulence in an
38 invertebrate model of invasive *Aspergillus* infection.

39

40 **Introduction:**

41 *Aspergillus fumigatus* (AF), in the genus *Aspergillus*, is the leading cause of invasive
42 pulmonary aspergillosis (IPA) (1). It is ubiquitous in nature and mainly affects people with a
43 compromised immune system. Factors such as prolonged neutropenia, hematologic
44 malignancy, and prolonged use of corticosteroids have all been linked to the disease;
45 however, patient populations with mild or no immunosuppression are increasingly
46 becoming susceptible (2, 3). The azole class of drugs is the primary choice and frontline
47 treatment for management of IPA that includes voriconazole, posaconazole, itraconazole
48 and isavuconazole (4). However, the recent rise in azole resistance raised the global alarm,
49 resulting in the WHO identifying drug-resistant AF as a pathogen of critical concern (5).
50 Azole drugs work by interacting with and blocking the Cyp51 enzyme, a Sterol 14α-
51 demethylase enzyme, that is part of ergosterol biosynthesis, the primary sterol in AF
52 membrane (6). However, binding affinities of azoles to Cyp51 differ on the basis of their
53 side-chains (7), and mutations in the Cyp51 protein sequence, along with duplication in the
54 promoter region, are the primary resistance mechanisms (8). Different mutations within
55 Cyp51 have been found to affect how drug binding occurs. For example, the G54 mutation
56 in Cyp51 confers resistance to itraconazole and posaconazole but not to voriconazole (9,
57 10). Structural studies have identified differential binding of the short-tail (voriconazole) vs.
58 long-tail (posaconazole and itraconazole) azole drugs to mutated Cyp51 as the reason for
59 the lack of cross-resistance (11). Further, MIC changes for posaconazole and itraconazole
60 correlate owing to their structure (12, 13). Drug binding to the target enzyme is and has
61 been defined as a major contributing factor to drug resistance. However, recently, non-

62 genetic changes including persistence, tolerance and hetero-resistance are also
63 associated with fungal response to azole drugs (14–16).

64 Iron and redox homeostasis play an important role in azole drug response (17).
65 Fungal mitochondria play an important role in regulating both these responses, as
66 mitochondrial dysfunction mutants are resistant to anti-fungal drugs (18–20). For example,
67 the mitochondrial iron transport gene, *mrsA*, is essential to maintain iron homeostasis and,
68 upon deletion, leads to abnormal levels of reactive oxygen species and is essential for
69 azole response (18). Iron homeostasis, oxidative stress response, and ergosterol
70 production are all linked to virulence (21). However, whether non-genetic mechanisms
71 regulate these phenotypes remains not fully understood.

72 Long non-coding RNAs (lncRNAs) are becoming increasingly important in regulating
73 non-genetic stress response mechanisms, including drug responses (22). In AF, we
74 previously showed that an lncRNA, *afu-182*, plays a role in fungal response to azole drugs
75 without a change in its minimum inhibitory concentration (16), where others have also
76 shown a role of ncRNA in drug resistance (23). To test the roles of lncRNAs in iron and
77 oxidative stress response, we analyzed the publicly available dataset (17, 24) and identified
78 that lncRNA *afu-254* was downregulated under oxidative and iron stress individually, and
79 ~90% downregulated in the presence of both stresses. Thus, we hypothesized that *afu-254*
80 is important for fungal response to oxidative stress, iron stress and azole response. *afu-254*
81 has previously been identified via a cDNA approach, and is annotated as a 171bp RNA (24,
82 25), below the threshold (of 200bp) to be classified as lncRNA (22).

83 Here, using rapid amplification of cDNA ends (RACE), we show that *afu-254* is an
84 854bp RNA with a 60 bp intron that plays a role in oxidative stress response and
85 differentially regulates azole response to long-tail azoles. In addition, *afu-254* is required
86 for virulence in an invertebrate model of invasive aspergillosis. Thus, here we characterize
87 an lncRNA that regulates fungal azole response and does not provide cross-resistance to
88 azoles. Future research will determine the *afu-254* interactome mediating these
89 phenotypes.
90

91 **Results:**

92 ***afu-254* is an 854bp-long non-coding RNA:**

93 To determine the roles of lncRNA in AF stress response, we identified *afu-254* to be
94 differentially regulated when exposed to oxidative and low iron stress (17). However, *afu-*
95 *254* is currently annotated as 145bp ncRNA (Af293 FungiDB accession no. Afu7g04115)
96 (24). To determine the role of *afu-254*, we first identified the boundaries of *afu-254*. We
97 performed 5' Rapid Amplification of cDNA ends (RACE) and 3' RACE (26). We demonstrated
98 that *afu-254* is a 854 bp lncRNA (sequence-region scf_000008_A_fumigatus_A1163
99 920,444 – 921 357, crick strand) with a 60bp intron (sequence-region
100 scf_000008_A_fumigatus_A1163 920,713– 920,772; crick strand) with a Fickett score of
101 0.39969 and a coding probability of 0.0317573 (27, 28), thus classifying it as a lncRNA
102 (Figure 1 and Figure S1).

103 ***afu-254* is differentially regulated by oxidative stress and regulates oxidative stress**
104 **response in AF:**

105 To confirm the differential expression of *afu-254*, we determined the RNA levels of *afu-254*
106 in GMM and GMM + H_2O_2 (3mM) via quantitative RT-PCR. We observed an 85% reduction
107 ($p<0.001$) in *afu-254* RNA levels in the presence of oxidative stress (Figure 1B). To determine
108 the role of *afu-254*, we generated a deletion strain (Δ*afu-254*) and complemented the strain
109 ectopically. We also over-expressed *afu-254* using the *gpdA* promoter from *A. nidulans* as
110 previously described (16). To confirm these strains were correct, we used qPCR to
111 determine the RNA levels of *afu-254* in each strain. We show that there is 4-fold over-

112 expression in the OE-254 strain and no RNA was detected in the Δ*afu-254* strain (Figure S2).
113 We also performed a northern blot to confirm the presence of RNA in the complement
114 strain (Figure S2). To determine the role of *afu-254* in regulating fungal response to oxidative
115 stress, we inoculated strains in top agar as previously described (29), punched a hole in the
116 center upon solidification, and added either 5mM H_2O_2 or 2mM menadione. We incubated
117 the plates for 36 hours and measured the zone of inhibition. Both Δ*afu-254* ($p<0.01$) and
118 OE-254 ($p<0.01$) showed increased zone of inhibition compared to WT, indicating *afu-254* is
119 necessary for AF to ameliorate oxidative stress (Figures 1C and 1D). The complement strain
120 reverted growth back to WT. Importantly, the OE-254 strain, like Δ*afu-254* strain, showed
121 increased susceptibility to oxidative stress. Using a spot assay, by plating AF conidia in the
122 presence of 3mM H_2O_2, we obtained similar results, further confirming the phenotype
123 (Figure S2). Thus, *afu-254* plays an important role in regulating fungal oxidative stress
124 response.

125 **Overexpression of *afu-254* forms a higher order structure leading to an antimorph:**
126 Δ*afu-254* strain shows significant growth inhibition in the presence of oxidative stress
127 compared to WT (Figure 1C and 1D). Interestingly, the OE-254 strains also showed severe
128 growth attenuation. To confirm the presence of *afu-254* in the OE-254 strain and to
129 determine if the stochiometric levels of *afu-254* are important for its functions, we did a
130 northern blot to determine the quantity and quality of *afu-254* transcript. We demonstrate
131 over-expression in the OE-254 mutant; however, we consistently observed the presence of
132 a band above the expected band of OE-254 (Figure 2A, red arrow). To confirm that the
133 higher order structure is not just a technical artifact due to the increased amount of target

134 RNA present in the solution, we loaded increasing amounts of WT RNA from 10-40μg
135 (Figure 2A). We did not see the higher-order structure at any level of loaded RNA, indicating
136 the second higher band is not an artifact. To identify if this second band is a higher order
137 structure, we heated the samples at 98°C for 15 min and cooled them immediately before
138 gel loading. As evident in Figure 2B, we saw complete denaturation of the higher molecular
139 band, and an increase in the weight of the expected monomeric RNA molecule, indicating a
140 possible higher ordered state with *afu-254* acting as an antimorph when over-expressed,
141 resulting in the same oxidative stress phenotype as the deletion mutant.

142 ***afu-254* regulates posaconazole and itraconazole response but is dispensable for**
143 **voriconazole response:**

144 We have previously shown that AF lncRNA regulates fungal response to azole drugs (16).
145 Others have shown that oxidative stress response plays a role in azole response (18, 30).
146 Thus, we inoculated WT, Δ*afu-254*, Comp-254 and OE-254 strains in the presence or
147 absence of posaconazole (0.03μg/ml), itraconazole (0.075 μg/ml), and voriconazole
148 (0.2μg/ml). In the presence of posaconazole, Δ*afu-254* strain is 73% more inhibited
149 compared to WT (Figure 3B and 3C, $p<0.0001$, One-Way ANOVA), and the OE-254 strain
150 failed to grow (Figure 3B and 3C, $p<0.0001$, One-Way ANOVA). Similarly, we saw a 74%
151 reduction in the Δ*afu-254* strain in the presence of itraconazole (Figure 3D and 3E,
152 $p<0.0001$, One-Way ANOVA) and like posaconazole, the OE-254 strain failed to grow in the
153 presence of itraconazole (Figure 3D and 3E, $p<0.0001$, One-Way ANOVA). Importantly, no
154 change in voriconazole susceptibility was observed (Figure S3A). Additionally, the

155 minimum inhibitory concentration of azoles did not change as measured by the broth
156 microdilution method (Figure S3B). To confirm this is not the growth stage specific
157 response, we grew the strains as liquid shaking cultures without or with 0.03μg/ml
158 posaconazole and weighed the 24-hour dry biomass. Both Δ*afu-2*54 and OE-254 strains
159 failed to produce biomass under liquid shaking conditions (Figure S3C), indicating the
160 azole susceptibility is not growth condition specific.

161 ***afu-254* regulates surface attachment and is important for azole response in surface**
162 **attached cultures:** To determine if germination is affecting the azole susceptibility
163 phenotypes of *afu-254*, we grew the strains in 24-well plates and allowed the biofilms to
164 develop for 12 hours. After biofilm formation, planktonic cells were washed with PBS and
165 GMM without or with 0.2μg/ml of posaconazole was added to the wells for 8 hours. The
166 wells are washed and stained with crystal violet to determine the attached biomass. The
167 OE-254 strain showed a 63% decrease in surface attachment after 20 hours in the absence
168 of azoles (Figure 3F, $p<0.0001$). Upon treatment with posaconazole, we normalized the
169 biofilms to untreated controls and observed a 25% reduction in Δ*afu-254* biofilms (Figure
170 3G, $p<0.01$, One-way ANOVA) and 78% reduction in OE-254 biofilms (Figure 3G, $p<0.0001$,
171 One-Way ANOVA) compared to WT. Thus, *afu-254* plays a role in surface attachment and
172 azole response of surface-attached cultures.

173 ***afu-254* regulates cell wall stress response:** Hydrogen peroxide-mediated oxidative
174 stress pathway leads to changes in the cell wall integrity pathway (31). Thus, to determine if
175 *afu-254* plays a role in fungal response to cell wall stress, we incubated the strains in the

176 absence and presence of Congo red, an anionic azo dye that affects cell wall rigidity (32).
177 Δ*afu-254* showed 54% reduction in growth ratio (Figures 4A and 4B, $p<0.0001$, One-Way
178 ANOVA); whereas OE-254 strain showed 40% reduction in growth ratio (Figures 4A and 4B,
179 $p<0.0001$, One-Way ANOVA) compared to WT strains. We did not see a difference when
180 strains were incubated with the echinocandin drug, Caspofungin, indicating a more
181 regulated cell wall stress response (Figure 4C).

182 **OE *afu-254* regulates macrophage uptake and killing *ex vivo*:** Reactive oxygen species
183 are detrimental to AF conidia and are a major weapon used by innate immune cells,
184 including macrophages, to kill AF conidia (33, 34). As *afu-254* plays a role in oxidative stress
185 response, we tested the ability of immortalized bone-marrow derived macrophages
186 (BMDMs) to engulf and/or kill conidia using an *ex vivo* adapted FLARE assay and CFU
187 plating assay, respectively (35). For uptake and killing, we incubated conidia from each
188 strain with BMDMs (MOI 5:1) for 3 or 5 hours, respectively. Interestingly, we observe a
189 decrease in uptake of Δ*afu-254* conidia compared to WT but not OE-254 conidia (Figure 4B,
190 $p<0.05$, Kruskal-Wallis test). We also observe a significant increase in OE-254 conidia
191 killing (Figure 5C, $p<0.0001$, Kruskal-Wallis test). The *ex vivo* killing of Δ*afu-254* trends
192 higher than WT but is not statistically significant (Figure 5C, $p=0.3616$, Kruskal-Wallis test).

193 ***afu-254* regulates fungal virulence in the *Galleria mellonella* model of infection:**

194 The ability to deal with oxidative stress and differences in cell wall stress response has
195 been associated with virulence (36, 37). Thus, we determined the virulence of AF strains in
196 the *G. mellonella* infection model (38). Worms infected with Δ*afu-254* had a median

197 survival time of 82 hours compared to 45.5 hours for WT (Figure 5D, $p<0.0001$, log rank

198 test). Fifty percent of larvae survived in the Δ*afu-254* group compared to 5% survival in the

199 WT group ($p< 0.001$, Figure 5D). On the other hand, 70% larvae infected with the OE-254

200 strain survived compared to WT (Figure 5D, median survival time – NA, $p<0.0001$, log-rank

201 test). The experiment was repeated three times with similar results. Thus, *afu-254* is

202 indispensable for fungal virulence.

203

204 **Discussion:**

205 Long non-coding RNAs play an important role in stress response in all forms of life, and
206 recent findings have shown their importance in azole response in AF (16, 23). However,
207 whether lncRNAs play a role in modulating other stresses is not entirely known. To
208 understand the role of lncRNAs in pathogenesis related stress response, we analyzed a
209 previously published transcriptome dataset in the absence or presence of oxidative stress,
210 low-iron stress, and a combination of both stresses (17). Based on the previous
211 transcriptomics results and our qPCR data, we determined that non-coding RNA *afu-254* is
212 highly expressed RNA and shows an 85% reduction in the presence of oxidative stress
213 mediated by H_2O_2 (Figure 1B). However, *afu-254* was predicted to be a 171bp ncRNA, failing
214 to meet the threshold of 200bp to be classified as lncRNA (24, 25). Previously, the ncRNAs
215 in AF were determined by a cDNA approach, and more recently, during the course of this
216 study, a genome wide characterization of lncRNAs in AF was reported (23, 25). Importantly,
217 *afu-254* was not characterized as an lncRNA in either of those studies; however, longer
218 RNA transcripts are predicted at the locus (24). We did a 5' and 3' RACE analysis and
219 characterized *afu-254* as an 854bp long ncRNA, and the DNA sequence coding for this
220 ncRNA contains a 60bp intron in the DNA sequence (Figure 1A and S1). Under the
221 conditions tested, we only found one transcript; however, whether splicing variants exist or
222 play a role in stress response or virulence is currently under investigation. Also, 5' RACE is
223 dependent on the ability of reverse transcriptase to amplify full length cDNA (39); and, it is
224 plausible that there is premature elongation termination. However, complementing *afu-254*
225 fragment ectopically reverts the oxidative stress phenotype, cell wall stress phenotype and

226 virulence back to the WT levels (Figures 3, 4 and 5), indicating functionality. Using species-
227 neutral computational models, the *afu-254* transcript is not predicted to be a protein-
228 coding sequence (27) and thus is classified as an lncRNA.

229 As our identification and confirmation showed *afu-254* to be differentially regulated by
230 oxidative stress, we grew the strains in the presence and absence of H_2O_2 and menadione,
231 which produce peroxide and superoxide, respectively. Both Δ*afu-254* and OE-254 strains
232 showed significant reduction compared to WT (Figures 1C and 1D). Various instances in AF
233 biology have shown the stochiometric levels of proteins to be important for their biological
234 function (40); however, this is the first instance where WT levels of an lncRNA are important
235 for its function in AF. To determine if OE-254 strain has a stable transcript, we did northern
236 blot analysis and observed the intact band at the expected size. In addition to the expected
237 band, we also saw a slow-moving band indicating either an *in-vitro* artifact, a multimeric
238 complex or a higher-order structure that is partially denatured (Figure 2A, red arrow).
239 LncRNAs assemble into three dimensional secondary structures like stem-loops and
240 cloverleaf, and structural conservation is important for their functions (41–43). Secondary
241 structures can coalesce to form higher order structures like pseudoknots, triplexes and G-
242 quadraplexes (44, 45). lncRNA can also interact with other RNAs, DNAs and proteins to
243 bind to chromatin to exert its function (46) . To determine if this is in fact a higher ordered
244 structure, we boiled the RNA at 98°C for 15 min, followed by rapid cooling on an ice bath
245 before gel loading. We saw an increase in the expected RNA band and a discernible loss of
246 the slow-moving band, indicating loss of higher ordered structure (Figure 2B); however, the
247 possibility that it is a DNA/RNA or RNA/RNA hybrid cannot be excluded. Overexpression of

248 lncRNA has long been associated with cancer development and metastasis (47, 48).
249 lncRNAs can act as sponges and decoys that can sequester other regulatory partners from
250 exerting their functions (49). For example, overexpression of lncRNA Xist serves as a
251 competing endogenous RNA (ceRNA) for miR-34a through sponging, leading to
252 overexpression of the MET oncogene that is involved in various cancers (50). In AF,
253 overexpression of *afu-254* ectopically acts as an antimorph presumably through the
254 formation of a non-functional multimeric form or tertiary structure (51). It is not clear if this
255 effect is due to *afu-254* driven by a constitutively active *gpdA* promoter or over-expression
256 in general. Further studies will focus on inducible promoters to fine-tune the *afu-254* levels
257 for structural and functional analysis.

258 Oxidative stress plays a role in fungal response to azole drugs (17). Previous studies on
259 lncRNAs have shown their roles in azole response (16, 23). Thus, we grew the strains in the
260 presence of voriconazole (short-tailed azole), posaconazole and itraconazole (long-tailed
261 azoles) (11). Surprisingly, we did not see a growth difference in response to voriconazole
262 (Figure S3A), but both Δ*afu-254* and OE-254 strains were hypersusceptible to both
263 posaconazole and itraconazole (Figure 3). We have previously shown that lncRNA *afu-182*
264 regulates pan-azole response (16); however, unlike *afu-182*, *afu-254*'s response is limited to
265 long-tailed azoles only. Previous studies have shown a strong correlation between
266 posaconazole and itraconazole susceptibility attributed to their structural similarities (12,
267 52). Azole cross-resistance in AF is determined by specific mutations in the Cyp51
268 sequence. For example, G54 and P216 mutations in Cyp51 result in resistance to
269 posaconazole and itraconazole but not to voriconazole (10, 53). The G448S mutation

270 provides a high level of resistance to voriconazole, but a low level of resistance to
271 posaconazole and itraconazole (54), and amino acid variations at M220 leads to pan-azole
272 resistance (55). Promoter duplication, along with amino-acid substitutions, is also a major
273 driver of pan-azole resistance (8). However, this is the first instance of a lncRNA regulating
274 variable response against short-tailed voriconazole and long-tailed azoles, posaconazole
275 and itraconazole. If this effect is mediated by a direct role in drug-*Cyp51* interaction or by
276 modulating *cyp51* gene expression is an area of further research. However, we show that
277 both deletion and overexpression of *afu-254* (Δ*afu-254* and OE-254 strains) play a role in
278 fungal response to azole drugs.

279 We also determined the role of *afu-254* in modulating cell-wall stress response. We plated
280 the strains in the presence of Congo red, an anionic azo dye that binds to chitin and blocks
281 the interaction between chitin and β1,3 glucans, thereby weakening the cell wall (32). We
282 saw both Δ*afu-254* and OE-254 strains showing increased susceptibility to Congo red
283 (Figure 4A), however, no difference was observed in response to Echinocandin drug
284 Caspofungin that targets 1-3-β-D-glucan synthase enzyme, *fksA* (56, 57). It is possible that
285 *afu-254* modulates the levels of cell wall macromolecules or only affects chitin and not
286 β1,3,-glucans. However, the cell wall is the primary interaction site for AF with immune
287 cells, which function via oxidative and non-oxidative mechanisms for fungal conidia killing.
288 As *afu-254* plays a role in mediating oxidative stress response, we performed an *ex vivo*
289 uptake and killing assay using BMDMs. Our data show decreased uptake but efficient
290 killing of Δ*afu-254* conidia, and increased killing of OE-254 conidia by BMDMs (Figure 5).
291 Even though we do see a similar trend in phenotypes in Δ*afu-254* and OE-254 strains, it is

292 possible that due to the higher order structure of the OE-254 strains, the antimorph effect
293 is beyond the phenotypes detected here, and we are currently parsing out these responses.
294 It is possible that an antimorphic allele in the OE-254 strain affects genomic loci with
295 similar functions, resulting in a hypersusceptible phenotype compared to the null mutant
296 (58). As we only observed cell wall stress phenotype in the presence of chitin-interacting
297 Congo red but not Caspofungin, it is possible that cell wall composition is slightly different
298 in Δ*afu-254* and OE-254 strains. Cell wall beta-glucan becomes exposed in swollen and
299 germinating spores and is recognized by Dectin-1 on resident alveolar macrophages (59).
300 This interaction leads to pro-inflammatory cytokine release (60); whereas chitin recognition
301 is immunomodulatory (61). Chitin can shift the immune response from a Th1 to Th2 and
302 can suppress the activity of IL-1 via increased secretion of IL-1Ra (61, 62). In Δ*afu-254* and
303 OE-254, it is possible that different levels of chitin and β glucans are exposed, leading to
304 differential immune response.

305 Thus, to further understand if the *ex vivo* immune response plays a role in virulence, we
306 used the *Galleria mellonella* model of infection, which has been used as a heterologous
307 host to study host-pathogen interaction (38). Here, we infected the larvae with the WT,
308 Δ*afu-254*, Comp-254 and OE-254 strains of AF. We observed significantly reduced mortality
309 in larvae infected with Δ*afu-254* and OE-254 strains that correlate with the *ex vivo* data
310 (Figure 5D). It is important to note that catalase-deficient mutants and superoxide
311 dismutase mutants that detoxify peroxides and superoxide, respectively, do not show
312 virulence defects in animal models (63, 64); whereas, oxidation resistance protein 1 (OxrA)
313 leads to virulence attenuation (65). It is well established that AF has a diverse set of

314 mechanisms to detoxify ROS; however, what genes, if any, are regulated by *afu-254* is not
315 clear. In the future, we plan to study the whole transcriptome response in Δ*afu-254* and OE-
316 254 strains compared to the WT strain.

317 In conclusion, we identified that *afu-254* is a long non-coding RNA that plays a role in
318 fungal response to oxidative stress, cell wall stress and virulence. Additionally, *afu-254*
319 modulates fungal azole response to posaconazole and itraconazole but not voriconazole
320 both in surface and attached cultures. The exact mechanisms of this lack of cross-
321 resistance phenomenon are not clear, and further investigations, both technical and
322 mechanistic, are required to study and understand the roles of lncRNAs in regulating fungal
323 azole response.

324

325

326 **Materials and Methods:**

327 **Rapid amplification of cDNA ends (RACE).** 5' RACE was done using 5' RACE system for
328 rapid amplification of cDNA ends from Invitrogen. Briefly, total RNA was isolated from
329 CEA10 strain as previously described (16). Gene specific primer, SD284, was used for first
330 strand synthesis. cDNA was tailed with dCTP and was amplified with UAP (from the kit) and
331 SD366.

332 3' RACE was done as previously described. Briefly, first strand cDNA was synthesized using
333 the Superscript II enzyme with primer Qt. *afu-254* was amplified with primers Q_0 and SD78.

334 The resulting fragments were ligated into the pJET1.2 vector (Thermo Fisher) and were
335 sequenced.

336 **Strain generation:** All strains and primers used in this study are listed in Supplementary
337 Table 1 and Supplementary Table 2 respectively. CEA17, a uridine/ uracil auxotrophic
338 derivative of CEA10 was used as host strain for creating the *Δafu-254 strain* used in this
339 study (66). Briefly, a 1kb region upstream and downstream of the predicted *afu-254*
340 sequence was amplified using primers SD266 and SD267 and SD218 and SD219. A
341 fragment encoding the 5'-orotodine decarboxylase gene from *A. parasiticus* was amplified
342 from pSD38.1 using primers SD1 and SD2. The three resulting fragments were fused via
343 PCR using primers SD222 and SD437.

344 To obtain the complement *afu-254* plasmid, DNA fragment corresponding to the *afu-254*
345 transcript was amplified with primers SD580 and SD581 that harbor AscI and Not1
346 restriction sites respectively. The resulting PCR fragment was digested with AscI and NotI

347 and was ligated into plasmid BS311 harboring the hygromycin resistance gene that was
348 previously digested with AscI and NotI (16).

349 To generate an over-expression strain, *A. nidulans gpdA* promoter just before the TSS was
350 amplified using primers SD134 and SD103 using *A. nidulans* gDNA as the template(67). The
351 DNA sequence corresponding to *afu-254* transcript was amplified using SD 468 and SD202
352 with AF gDNA as the template. These fragments were fused together via fusion PCR using
353 primers SD136 and SD323 that harbor AscI and NotI sites. The resulting fragment was
354 ligated into plasmid pSD18.1, which contains the *pyrG* gene as a fungal selection marker,
355 previously digested with AscI and NotI.

356 DNA was transformed into the protoplast using polyethylene glycol mediated
357 transformation as previously described (68).

358 **Quantitative RT PCR:** RNA was isolated as described previously (69). For RT-qPCR, 1 μg of
359 RNA was used for first-strand synthesis using MMLV-reverse transcriptase (Promega) per
360 the manufacturer's instructions. Second-strand synthesis and quantitative real-time PCR
361 were performed using iTaq Universal SYBR mix (BioRad) in the CFX Connect Real-Time
362 System (BIO-RAD). *afu-254* transcript levels were quantified using primers SD 324 and SD
363 325. Histone H4 was used for normalization, and transcript levels were quantified using
364 primers SD 375 and SD 376.

365 **Northern Analysis:** For northern analysis, indicated amounts of RNA was loaded onto
366 1.2% agarose – 2.2M formaldehyde gel and blotted on positively charged nylon membrane.

367 DIG labelled probe were synthesized with primers SD201 and SD188 using PCR DIG probe
368 synthesis kit per manufacturer's recommendations.

369 **Stress test:** To test the role of *afu-254* in oxidative stress, cell membrane stress and cell
370 wall stress response in AF, serial spore dilutions of indicated strains were prepared and
371 inoculated on the plate containing indicated stresses along with no stress control for 48
372 hours at 37°C, 5% CO_2. Colony diameter was measured, and statistical analysis was
373 performed using GraphPad Prism.
374 Punch hole assay was performed as previously described (40). Briefly, 10^5 spores per ml in
375 5ml of top agar were plated on GMM plates. After solidification, a filter pipette tip (200µL)
376 was used to core out the centre of the plate. 100µl of either 5% H_2O_2 or 2mM Menadione
377 were added and zone on inhibition was measured.
378 All experiments were performed in triplicate and were repeated three times.

379 **Broth microdilution assay to determine minimum inhibitory concentration:** Spore
380 suspensions were adjusted to 5 x 10^5 spores per ml and 100µl of spores was added to
381 100µl of drug in GMM in a 96 well plate (16µg/ml – 0.0156µg/ml). The first well showing no
382 fungal growth was recorded as MIC.

383 **Biofilm assay:** In a 24-well plate, 1 ml of GMM containing 10^5 spores of Af strains was
384 added. The plates were centrifuged at 250 g for 10 minutes and incubated at 37°C for
385 twelve hours. The culture supernatant was removed, and wells were washed twice with
386 PBS and stained with 2 ml of 0.1% crystal violet for 10 min. GMM without or with 0.2µg/ml
387 of posaconazole was added for 8 hours. Wells were then washed twice using autoclaved

388 water to remove excess Crystal violet and treated with 1.5 ml of 100% ethanol for 10
389 minutes. 75 µl of suspension from each well was transferred to the 3 wells of 96 well plate,
390 and absorbance at 600 nm was read using a MultiSkan Sky High Microplate
391 Spectrophotometer. To calculate biofilm formation, the background reading was
392 subtracted from the test reading. For azole treated samples, the absorbance was
393 normalized to untreated controls.

394 ***Ex vivo* killing Assay:** Immortalized C57BL/6 BMDMs (BEI resources; NR-9546) were used
395 for the macrophage killing assay. Briefly, BMDMs were plated at $0.5x10^6$ cells/well in a 12-
396 well plate. The next day conidia from the indicated strains, at a ratio of 5:1 (conidia:cells),
397 were added to the BMDMs, centrifuged at 1000rpm for 2 minutes, and then incubated for 5
398 hours at 37°C, 5% CO_2. Following incubation, cells were lysed for 2 minutes using ice-cold
399 water. Serial dilutions of the wells were made in PBS and plated on GMM plates. Plates
400 were incubated at 37°C for 48 hours and CFUs were counted.

401 **Macrophage uptake assay:** BMDMs were plated at $0.5x10^6$ cells/well in a 12-well plate.
402 The next day, conidia biotinylation protocol from (35) was used to label each strain with
403 AF633. Briefly, conidia from each of the 4 strains were rotated in Biotin-XX, SSE at a final
404 concentration of 5µg/ml in 50 mM carbonate buffer for 1 hr. Following incubation, unbound
405 biotin was neutralized using 0.1 M Tris- HCL and rotated at room temperature for 15
406 minutes. Conidia were then resuspended in PBS with 0.02 mg/ml of AF633, incubated for
407 45 minutes with constant rotation, and protected from light until experimental use.
408 Following labeling, each of the 5 biotinylated strains were added to the corresponding wells

409 at a ratio of 5:1 (conidia: cell) and incubated for 3 hours at 37°C, 5% CO_2. After incubation,
410 wells were washed with PBS and suspended in FACs buffer. Wells were gently scraped with
411 a cell scraper to resuspend BMDMs. Cells were stained with DAPI for L/D detection and
412 were analyzed using the BD LSR II flow cytometer. Gating on BMDM uptake (AF633+) vs.
413 empty BMDMs (AF633-) was used to quantify total uptake and percentage of BMDM uptake
414 for each strain. Data for CFU and Uptake represent combined data from 3 experiments
415 (each with 4-5 replicates) and were analyzed with Prism (v10.4.1) using one-way ANOVA
416 with the Kruskal-Wallis test with Dunn's multiple comparisons.

417 ***Galleria mellonella* infection:** A total of 20 *Galleria mellonella* larvae of cream-white color
418 and similar size were used per strain of AF. Ten µl containing $5x10^4$ spores was injected
419 directly via Hamilton syringe to the hemocoel as previously described (38). 10 µl of PBS
420 was administered to the control group to ensure PBS was free from contamination.
421 Additionally, 10 worms that were neither infected nor stabbed were used as a control to
422 check for the quality of the worms. After injection, larvae were incubated at 37°C until 5
423 days. For survival analysis, larvae were monitored 3 times daily post-injection. The death of
424 larvae was ensured by a lack of movement upon physical stimuli. Statistical analysis was
425 performed using GraphPad Prism software. The experiment was done three times with
426 similar results.
427

428 **Statistical Analyses**: Non-parametric tests were used for *ex vivo* assay and virulence

429 assay. Parametric tests were used for other comparisons. GraphPad Prism was used for all

430 statistical analyses. *$p<0.05$, ** $p<0.01$, ***$p<0.001$, ****$p<0.0001$

431

Acknowledgements:

We would like to acknowledge members of the Dhingra laboratory and the Eukaryotic Pathogen Innovation Center for discussions surrounding the experiments in the manuscript. The research in the Dhingra lab is supported by start-up funds from the Department of Biological Sciences at Clemson University and a National Institute of General Medical Sciences (NIGMS) award (P20GM146584) (PI - James Morris). The funding sources had no role in the study design, data collection and interpretation, preparation of this manuscript or the decision to submit the manuscript. We acknowledge the UC Merced Stem Cell Instrumentation Foundry for assistance in generating flow cytometry data.

References:

1. Earle K, Valero C, Conn DP, Vere G, Cook PC, Bromley MJ, Bowyer P, Gago S. 2023. Pathogenicity and virulence of Aspergillus fumigatus. Virulence 14:2172264.

2. Abers MS, Ghebremichael MS, Timmons AK, Warren HS, Poznansky MC, Vyas JM. 2016. A Critical Reappraisal of Prolonged Neutropenia as a Risk Factor for Invasive Pulmonary Aspergillosis. Open Forum Infect Dis 3:ofw036.

3. Tio SY, Chen SC-A, Hamilton K, Heath CH, Pradhan A, Morris AJ, Korman TM, Morrissey O, Halliday CL, Kidd S, Spelman T, Brell N, McMullan B, Clark JE, Mitsakos K, Hardiman RP, Williams P, Campbell AJ, Beardsley J, Van Hal S, Yong MK, Worth LJ, Slavin MA. 2023. Invasive aspergillosis in adult patients in Australia and New Zealand: 2017-2020. Lancet Reg Health West Pac 40:100888.

4. Patterson TF, Thompson GR, Denning DW, Fishman JA, Hadley S, Herbrecht R, Kontoyiannis DP, Marr KA, Morrison VA, Nguyen MH, Segal BH, Steinbach WJ, Stevens DA, Walsh TJ, Wingard JR, Young J-AH, Bennett JE. 2016. Practice Guidelines for the Diagnosis and Management of Aspergillosis: 2016 Update by the Infectious Diseases Society of America. Clin Infect Dis 63:e1–e60.

5. WHO fungal priority pathogens list to guide research, development and public health action. https://www.who.int/publications/i/item/9789240060241. Retrieved 19 September 2025.

461 6. Lee Y, Robbins N, Cowen LE. 2023. Molecular mechanisms governing antifungal drug
462 resistance. npj Antimicrob Resist 1:5.

463 7. Shi N, Zheng Q, Zhang H. 2020. Molecular Dynamics Investigations of Binding
464 Mechanism for Triazoles Inhibitors to CYP51. Front Mol Biosci 7:586540.

465 8. Dhingra S, Cramer RA. 2017. Regulation of Sterol Biosynthesis in the Human Fungal
466 Pathogen Aspergillus fumigatus: Opportunities for Therapeutic Development. Front
467 Microbiol 8:92.

468 9. Diaz-Guerra TM, Mellado E, Cuenca-Estrella M, Rodriguez-Tudela JL. 2003. A Point
469 Mutation in the 14α-Sterol Demethylase Gene cyp51A Contributes to Itraconazole
470 Resistance in Aspergillus fumigatus. Antimicrobial Agents and Chemotherapy 47:1120–
471 1124.

472 10. Vazquez JA, Manavathu EK. 2016. Molecular Characterization of a Voriconazole-
473 Resistant, Posaconazole-Susceptible Aspergillus fumigatus Isolate in a Lung
474 Transplant Recipient in the United States. Antimicrobial Agents and Chemotherapy
475 60:1129–1133.

476 11. Sagatova AA, Keniya MV, Tyndall JDA, Monk BC. 2018. Impact of Homologous
477 Resistance Mutations from Pathogenic Yeast on Saccharomyces cerevisiae Lanosterol
478 14α-Demethylase. Antimicrobial Agents and Chemotherapy 62:10.1128/aac.02242-17.

479 12. Mosquera J, Denning DW. 2002. Azole Cross-Resistance in Aspergillus fumigatus.
480 Antimicrob Agents Chemother 46:556–557.

481 13. Pfaller MA, Messer SA, Boyken L, Rice C, Tendolkar S, Hollis RJ, Diekema DJ. 2008. In
482 Vitro Survey of Triazole Cross-Resistance among More than 700 Clinical Isolates of
483 Aspergillus Species. J Clin Microbiol 46:2568–2572.

484 14. Scott J, Valero C, Mato-López Á, Donaldson IJ, Roldán A, Chown H, Rhijn NV, Lobo-Vega
485 R, Gago S, Furukawa T, Morogovsky A, Ami RB, Bowyer P, Osherov N, Fontaine T,
486 Goldman GH, Mellado E, Bromley M, Amich J. 2022. Aspergillus fumigatus can display
487 persistence to the fungicidal drug voriconazole. bioRxiv
488 https://doi.org/10.1101/2022.05.16.491816.

489 15. Scott J, Valero C, Mato-López Á, Donaldson IJ, Roldán A, Chown H, Rhijn NV, Lobo-Vega
490 R, Gago S, Furukawa T, Morogovsky A, Ami RB, Bowyer P, Osherov N, Fontaine T,
491 Goldman GH, Mellado E, Bromley M, Amich J. 2023. Aspergillus fumigatus Can Display
492 Persistence to the Fungicidal Drug Voriconazole. Microbiology Spectrum
493 https://doi.org/10.1128/spectrum.04770-22.

494 16. Poudyal NR, Mehlem RT, Doneparthi P, Cady T, Willger SD, Ortiz M, Noorai RE, Stajich
495 JE, Dhingra S. 2025. A long non-coding RNA regulates triazole antifungal susceptibility
496 and virulence in Aspergillus fumigatus. bioRxiv
497 https://doi.org/10.1101/2025.10.16.682787.

498 17. Kurucz V, Krüger T, Antal K, Dietl A-M, Haas H, Pócsi I, Kniemeyer O, Emri T. 2018.
499 Additional oxidative stress reroutes the global response of Aspergillus fumigatus to iron
500 depletion. BMC Genomics 19:357.

501 18. Long N, Xu X, Qian H, Zhang S, Lu L. 2016. A Putative Mitochondrial Iron Transporter
502 MrsA in Aspergillus fumigatus Plays Important Roles in Azole-, Oxidative Stress
503 Responses and Virulence. Front Microbiol 7.

504 19. Chen M, Zhong G, Wang S, Chen P, Li L. 2022. Deletion of cox7c Results in Pan-Azole
505 Resistance in Aspergillus fumigatus. Antimicrobial Agents and Chemotherapy
506 66:e00151-22.

507 20. Zhou X, Yang G, Li C, Yang F, Chang X. 2022. Requirement of a putative mitochondrial
508 GTPase, GemA, for azole susceptibility, virulence, and cell wall integrity in Aspergillus
509 fumigatus. Front Microbiol 13.

510 21. Haas H. 2012. Iron – A Key Nexus in the Virulence of Aspergillus fumigatus. Front
511 Microbiol 3:28.

512 22. Mattick JS, Amaral PP, Carninci P, Carpenter S, Chang HY, Chen L-L, Chen R, Dean C,
513 Dinger ME, Fitzgerald KA, Gingeras TR, Guttman M, Hirose T, Huarte M, Johnson R,
514 Kanduri C, Kapranov P, Lawrence JB, Lee JT, Mendell JT, Mercer TR, Moore KJ, Nakagawa
515 S, Rinn JL, Spector DL, Ulitsky I, Wan Y, Wilusz JE, Wu M. 2023. Long non-coding RNAs:
516 definitions, functions, challenges and recommendations. Nat Rev Mol Cell Biol 24:430–
517 447.

518 23. Bowyer P, Weaver D, Qi T, Chown H, Fraczek M, Lebedinec R, Dineen L, Valero C, Rhijn
519 N van, Furukawa T, Bromley M, Delneri D. 2025. Genome-wide discovery and

520 phenotyping of non-coding transcripts in A. fumigatus reveals lncRNAs with a role in
521 antifungal drug sensitivity https://doi.org/10.21203/rs.3.rs-6048166/v1.

522 24. Basenko EY, Shanmugasundram A, Böhme U, Starns D, Wilkinson PA, Davison HR,
523 Crouch K, Maslen G, Harb OS, Amos B, McDowell MA, Kissinger JC, Roos DS, Jones A.
524 2024. What is new in FungiDB: a web-based bioinformatics platform for omics-scale
525 data analysis for fungal and oomycete species. Genetics 227:iyae035.

526 25. Jöchl C, Rederstorff M, Hertel J, Stadler PF, Hofacker IL, Schrettl M, Haas H,
527 Hüttenhofer A. 2008. Small ncRNA transcriptome analysis from Aspergillus fumigatus
528 suggests a novel mechanism for regulation of protein synthesis. Nucleic Acids
529 Research 36:2677–2689.

530 26. Scotto–Lavino E, Du G, Frohman MA. 2006. 3' End cDNA amplification using classic
531 RACE. Nat Protoc 1:2742–2745.

532 27. Kang Y-J, Yang D-C, Kong L, Hou M, Meng Y-Q, Wei L, Gao G. 2017. CPC2: a fast and
533 accurate coding potential calculator based on sequence intrinsic features. Nucleic
534 Acids Res 45:W12–W16.

535 28. Wang L, Park HJ, Dasari S, Wang S, Kocher J-P, Li W. 2013. CPAT: Coding-Potential
536 Assessment Tool using an alignment-free logistic regression model. Nucleic Acids Res
537 41:e74.

538 29. Sugareva V, Härtl A, Brock M, Hübner K, Rohde M, Heinekamp T, Brakhage AA. 2006.
539 Characterisation of the laccase-encoding gene abr2 of the dihydroxynaphthalene-like
540 melanin gene cluster of Aspergillus fumigatus. Arch Microbiol 186:345–355.

541 30. Sasse C, Bastakis E, Bakti F, Höfer AM, Zangl I, Schüller C, Köhler AM, Gerke J,
542 Krappmann S, Finkernagel F, Harting R, Strauss J, Heimel K, Braus GH. 2023. Induction
543 of Aspergillus fumigatus zinc cluster transcription factor OdrA/Mdu2 provides
544 combined cellular responses for oxidative stress protection and multiple antifungal
545 drug resistance. mBio 14:e0262823.

546 31. Carrasco-Navarro U, Aguirre J. 2021. H2O2 Induces Major Phosphorylation Changes in
547 Critical Regulators of Signal Transduction, Gene Expression, Metabolism and
548 Developmental Networks in Aspergillus nidulans. Journal of Fungi 7:624.

549 32. Linder T. 2018. Evaluation of the chitin-binding dye Congo red as a selection agent for
550 the isolation, classification, and enumeration of ascomycete yeasts. Archives of
551 Microbiology 200:671.

552 33. Shlezinger N, Hohl TM. Mitochondrial Reactive Oxygen Species Enhance Alveolar
553 Macrophage Activity against Aspergillus fumigatus but Are Dispensable for Host
554 Protection. mSphere 6:e00260-21.

555 34. Hatinguais R, Pradhan A, Brown GD, Brown AJP, Warris A, Shekhova E. 2021.
556 Mitochondrial Reactive Oxygen Species Regulate Immune Responses of Macrophages
557 to Aspergillus fumigatus. Front Immunol 12.

558 35. Jhingran A, Mar KB, Kumasaka DK, Knoblaugh SE, Ngo LY, Segal BH, Iwakura Y, Lowell
559 CA, Hamerman JA, Lin X, Hohl TM. 2012. Tracing Conidial Fate and Measuring Host Cell
560 Antifungal Activity Using a Reporter of Microbial Viability in the Lung. Cell Rep 2:1762–
561 1773.

562 36. Zhai P, Shi L, Zhong G, Jiang J, Zhou J, Chen X, Dong G, Zhang L, Li R, Song J. 2021. The
563 OxrA Protein of Aspergillus fumigatus Is Required for the Oxidative Stress Response
564 and Fungal Pathogenesis. Applied and Environmental Microbiology 87:e01120-21.

565 37. Earle K, Valero C, Conn DP, Vere G, Cook PC, Bromley MJ, Bowyer P, Gago S.
566 Pathogenicity and virulence of Aspergillus fumigatus. Virulence 14:2172264.

567 38. Durieux M-F, Melloul É, Jemel S, Roisin L, Dardé M-L, Guillot J, Dannaoui É, Botterel F.
568 Galleria mellonella as a screening tool to study virulence factors of Aspergillus
569 fumigatus. Virulence 12:818–834.

570 39. Scotto–Lavino E, Du G, Frohman MA. 2006. 5' end cDNA amplification using classic
571 RACE. Nat Protoc 1:2555–2562.

572 40. Dhingra S, Andes D, Calvo AM. 2012. VeA regulates conidiation, gliotoxin production,
573 and protease activity in the opportunistic human pathogen Aspergillus fumigatus.
574 Eukaryot Cell 11:1531–1543.

575 41. Diederichs S. 2014. The four dimensions of noncoding RNA conservation. Trends in
576 Genetics 30:121–123.

577 42. Graf J, Kretz M. 2020. From structure to function: Route to understanding lncRNA
578 mechanism. BioEssays 42:2000027.

579 43. Novikova IV, Hennelly SP, Sanbonmatsu KY. 2012. Sizing up long non-coding RNAs.
580 Bioarchitecture 2:189–199.

581 44. Tassinari M, Richter SN, Gandellini P. 2021. Biological relevance and therapeutic
582 potential of G-quadruplex structures in the human noncoding transcriptome. Nucleic
583 Acids Res 49:3617–3633.

584 45. Wan Y, Kertesz M, Spitale RC, Segal E, Chang H. 2011. Understanding the transcriptome
585 through RNA structure. Nat Rev Genet 12:10.1038/nrg3049.

586 46. Statello L, Guo C-J, Chen L-L, Huarte M. 2021. Gene regulation by long non-coding
587 RNAs and its biological functions. Nat Rev Mol Cell Biol 22:96–118.

588 47. Baba SK, Baba SK, Mir R, Elfaki I, Algehainy N, Ullah MF, Barnawi J, Altemani FH, Alanazi
589 M, Mustafa SK, Masoodi T, Akil ASA, Bhat AA, Macha MA. 2023. Long non-coding RNAs
590 modulate tumor microenvironment to promote metastasis: novel avenue for
591 therapeutic intervention. Front Cell Dev Biol 11.

592 48. Liu L, Zhang Y, Lu J. 2020. The roles of long noncoding RNAs in breast cancer
593 metastasis. Cell Death Dis 11:749.

49. Gao N, Li Y, Li J, Gao Z, Yang Z, Li Y, Liu H, Fan T. 2020. Long Non-Coding RNAs: The Regulatory Mechanisms, Research Strategies, and Future Directions in Cancers. Front Oncol 10.

50. Yang J, Qi M, Fei X, Wang X, Wang K. 2021. Long non-coding RNA XIST: a novel oncogene in multiple cancers. Molecular Medicine 27:159.

51. Muller HJ. 1932. Further studies on the nature and causes of gene mutations.

52. Pfaller MA, Messer SA, Boyken L, Rice C, Tendolkar S, Hollis RJ, Diekema DJ. 2008. In Vitro Survey of Triazole Cross-Resistance among More than 700 Clinical Isolates of Aspergillus Species. Journal of Clinical Microbiology 46:2568–2572.

53. Ballard E, Melchers WJG, Zoll J, Brown AJP, Verweij PE, Warris A. 2018. In-host microevolution of Aspergillus fumigatus: A phenotypic and genotypic analysis. Fungal Genet Biol 113:1–13.

54. Pelaez T, Gijón P, Bunsow E, Bouza E, Sánchez-Yebra W, Valerio M, Gama B, Cuenca-Estrella M, Mellado E. 2012. Resistance to Voriconazole Due to a G448S Substitution in Aspergillus fumigatus in a Patient with Cerebral Aspergillosis. J Clin Microbiol 50:2531–2534.

55. Mellado E, Garcia-Effron G, Alcazar-Fuoli L, Cuenca-Estrella M, Rodriguez-Tudela JL. 2004. Substitutions at Methionine 220 in the 14α-Sterol Demethylase (Cyp51A) of Aspergillus fumigatus Are Responsible for Resistance In Vitro to Azole Antifungal Drugs. Antimicrob Agents Chemother 48:2747–2750.

614 56. Douglas CM, Foor F, Marrinan JA, Morin N, Nielsen JB, Dahl AM, Mazur P, Baginsky W, Li
615 W, el-Sherbeini M. 1994. The Saccharomyces cerevisiae FKS1 (ETG1) gene encodes an
616 integral membrane protein which is a subunit of 1,3-beta-D-glucan synthase. Proc Natl
617 Acad Sci U S A 91:12907–12911.

618 57. Kelly R, Register E, Hsu MJ, Kurtz M, Nielsen J. 1996. Isolation of a gene involved in 1,3-
619 beta-glucan synthesis in Aspergillus nidulans and purification of the corresponding
620 protein. Journal of Bacteriology 178:4381–4391.

621 58. Sijacic P, Wang W, Liu Z. 2011. Recessive Antimorphic Alleles Overcome Functionally
622 Redundant Loci to Reveal TSO1 Function in Arabidopsis Flowers and Meristems. PLoS
623 Genet 7:e1002352.

624 59. Steele C, Rapaka RR, Metz A, Pop SM, Williams DL, Gordon S, Kolls JK, Brown GD. 2005.
625 The Beta-Glucan Receptor Dectin-1 Recognizes Specific Morphologies of Aspergillus
626 fumigatus. PLoS Pathog 1:e42.

627 60. Batbayar S, Lee DH, Kim HW. 2012. Immunomodulation of Fungal β-Glucan in Host
628 Defense Signaling by Dectin-1. Biomol Ther (Seoul) 20:433–445.

629 61. Becker KL, Aimanianda V, Wang X, Gresnigt MS, Ammerdorffer A, Jacobs CW,
630 Gazendam RP, Joosten LAB, Netea MG, Latgé JP, van de Veerdonk FL. 2016. Aspergillus
631 Cell Wall Chitin Induces Anti- and Proinflammatory Cytokines in Human PBMCs via the
632 Fc-γ Receptor/Syk/PI3K Pathway. mBio 7:e01823-15.

633 62. Wagener J, Malireddi RKS, Lenardon MD, Köberle M, Vautier S, MacCallum DM,
634 Biedermann T, Schaller M, Netea MG, Kanneganti T-D, Brown GD, Brown AJP, Gow NAR.
635 2014. Fungal Chitin Dampens Inflammation through IL-10 Induction Mediated by NOD2
636 and TLR9 Activation. PLOS Pathogens 10:e1004050.

637 63. Paris S, Wysong D, Debeaupuis J-P, Shibuya K, Philippe B, Diamond RD, Latgé J-P. 2003.
638 Catalases of Aspergillus fumigatus. Infect Immun 71:3551–3562.

639 64. Lambou K, Lamarre C, Beau R, Dufour N, Latge J-P. 2010. Functional analysis of the
640 superoxide dismutase family in Aspergillus fumigatus. Molecular Microbiology 75:910–
641 923.

642 65. Zhai P, Shi L, Zhong G, Jiang J, Zhou J, Chen X, Dong G, Zhang L, Li R, Song J. The OxrA
643 Protein of Aspergillus fumigatus Is Required for the Oxidative Stress Response and
644 Fungal Pathogenesis. Appl Environ Microbiol 87:e01120-21.

645 66. Bertuzzi M, van Rhijn N, Krappmann S, Bowyer P, Bromley MJ, Bignell EM. 2020. On the
646 lineage of Aspergillus fumigatus isolates in common laboratory use. Med Mycol 59:7–
647 13.

648 67. Punt PJ, Dingemanse MA, Kuyvenhoven A, Soede RDM, Pouwels PH, van den Hondel
649 CAMJJ. 1990. Functional elements in the promoter region of the *Aspergillus nidulans*
650 *gpdA* gene encoding glyceraldehyde-3-phosphate dehydrogenase. Gene 93:101–109.

651 68. Szewczyk E, Nayak T, Oakley CE, Edgerton H, Xiong Y, Taheri-Talesh N, Osmani SA,
652 Oakley BR. 2006. Fusion PCR and gene targeting in Aspergillus nidulans. Nat Protoc
653 1:3111–3120.

654 69. Zepeda B, Verdonk JC. 2022. RNA Extraction from Plant Tissue with Homemade Acid
655 Guanidinium Thiocyanate Phenol Chloroform (AGPC). Current Protocols 2:e351.

656

657

Figure 1:

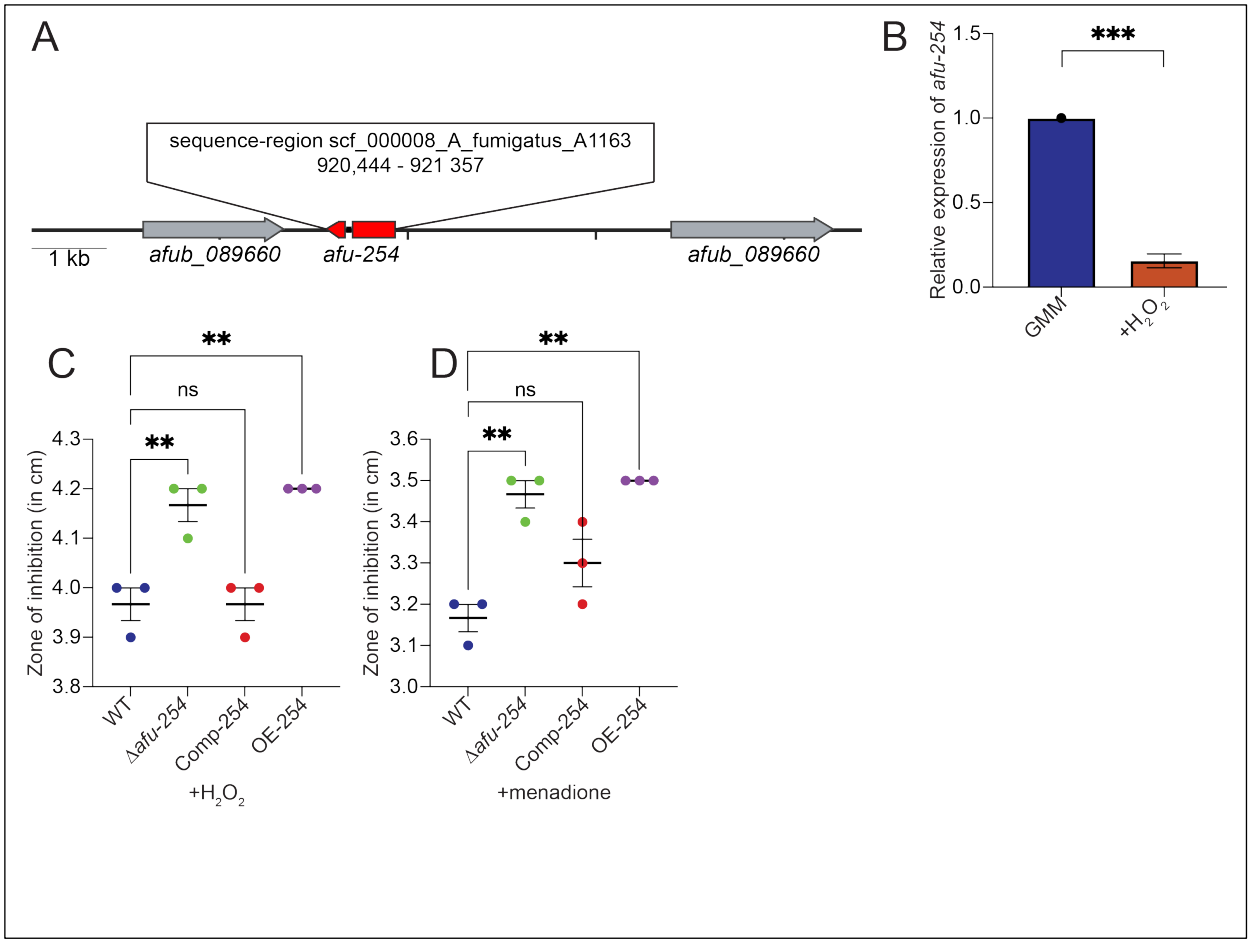

Figure 1. *afu-254* is an lncRNA that regulates fungal oxidative stress response. (A) 5' and 3' rapid amplification of cDNA ends confirmed the boundary of *afu-254* in the genome as indicated. (B) qPCR analysis showing the relative levels of *afu-254* in the presence of oxidative stress compared to GMM. Fungal strains were inoculated in top agar. After solidification, a core was cut in the center using a sterile pipette tip, and 100µl of either (C) 5mM H_2O_2 or (D) 2mM menadione was added. The zone of inhibition was measured after 36 hours and represented. ** $p<0.01$, *** $p<0.001$, ns – not significant

Figure 2:

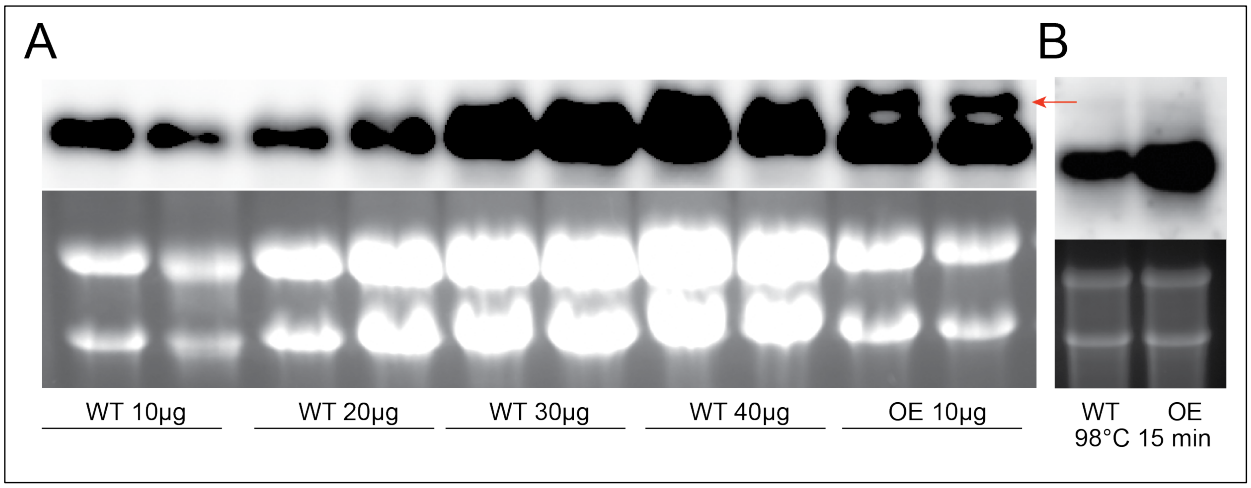

Figure 2. OE-254 constitutes an anamorph. (A) WT and OE-254 RNA were loaded in a denaturing formaldehyde gel at the indicated concentration. The samples were heated at 65°C for 5 min before loading. The OE-254 strain shows the presence of a higher molecular weight band (red arrow). (B) The samples were heated at 98°C for 15 mins, leading to loss of the higher molecular weight band.

Figure 3:

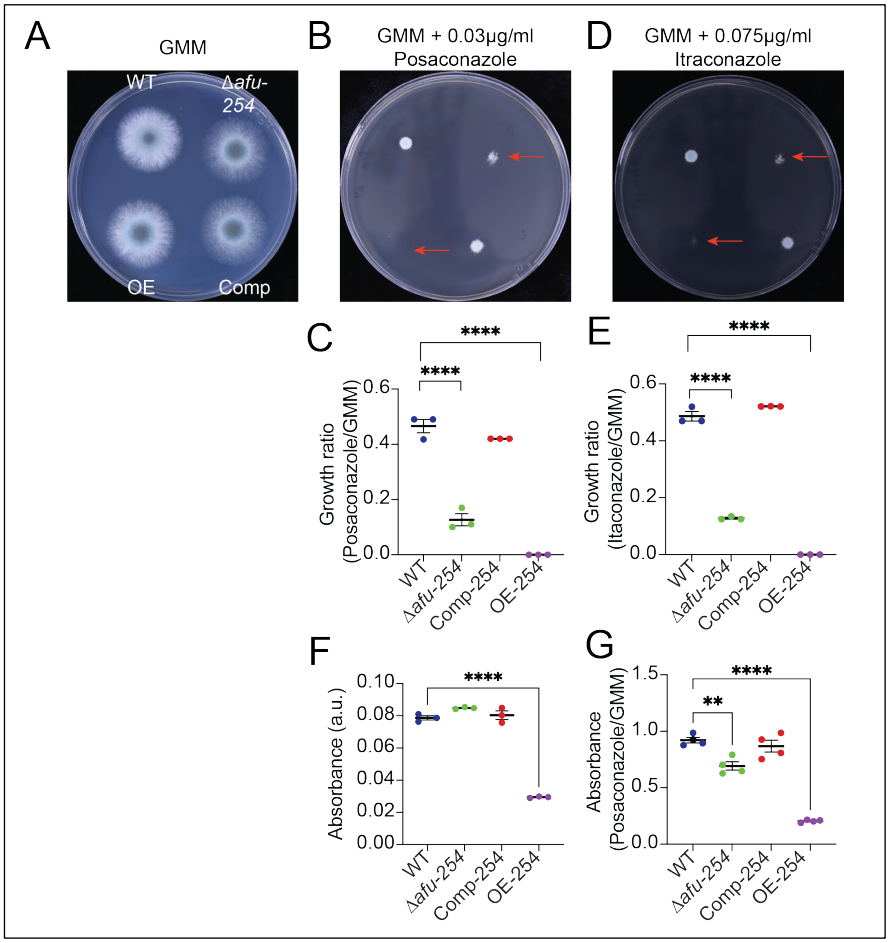

Figure 3. *afu-254* plays a role in fungal response to posaconazole and itraconazole on solid medium and surface attached cultures. Fungal strains were spot inoculated (10^4 spores) in (A) absence of drug or presence of (B and C) posaconazole or (D and E) Itraconazole. Both Δ*afu-254* and OE-254 show increased susceptibility to long tailed azoles. (D and E) Quantitative measurements of fungal growth after 48 hours are represented as a ratio of fungal growth in the presence and absence of the indicated drug. (F) *afu-254* plays a role in fungal surface attachment. Fungal strains were allowed to adhere to the abiotic surface for 12 hours. The surface attached cultures were then (F) left untreated (GMM), treated with posaconazole for 8 hours (GMM + 0.2µg/ml posaconazole), washed and stained with crystal violet. (F) Values represent the absorbance of untreated samples. The OE-254 strain shows decreased surface attachment. (G) Values represent the ratio between absorbance measured after azole treatment and fungal attachment before treatment at the 12-hour time point. a.u. – arbitrary units. **** $p<0.0001$, One-way ANOVA.

Figure 4:

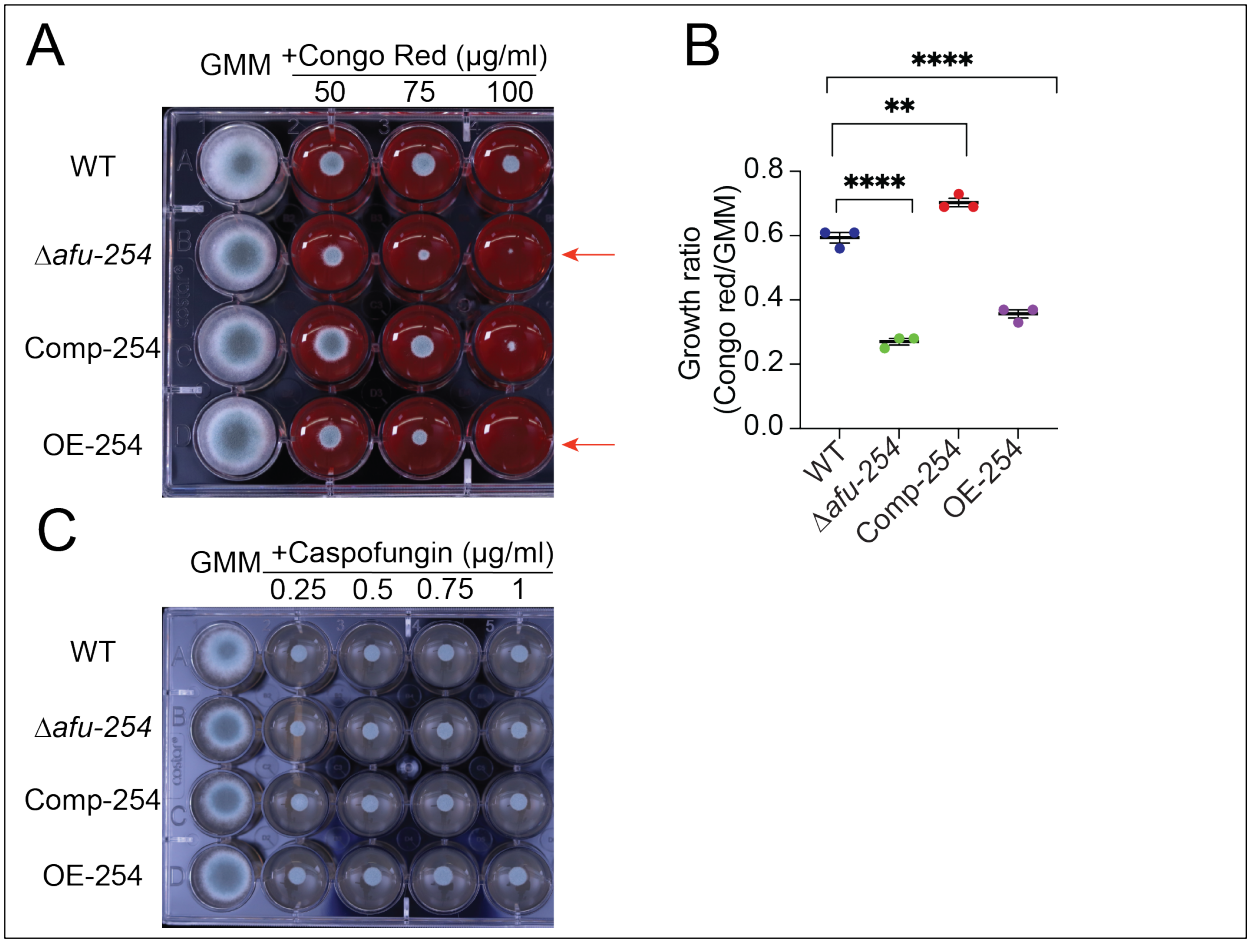

Figure 4. *afu-254* mediates fungal cell wall response to Congo red but not to Caspofungin. Fungal strains were spot inoculated (10^4 spores) in a 24 well plate in the absence or presence of indicated concentrations of (A) Congo red or (C). Caspofungin. Both Δ*afu-254* and OE-254 strains are susceptible to Congo red (red arrows) but not to Caspofungin. (B) Quantitative analysis of fungal growth is represented as a ratio between growth in the presence of CR and the absence of CR. ** $p<0.01$, **** $p<0.0001$.

Figure 5

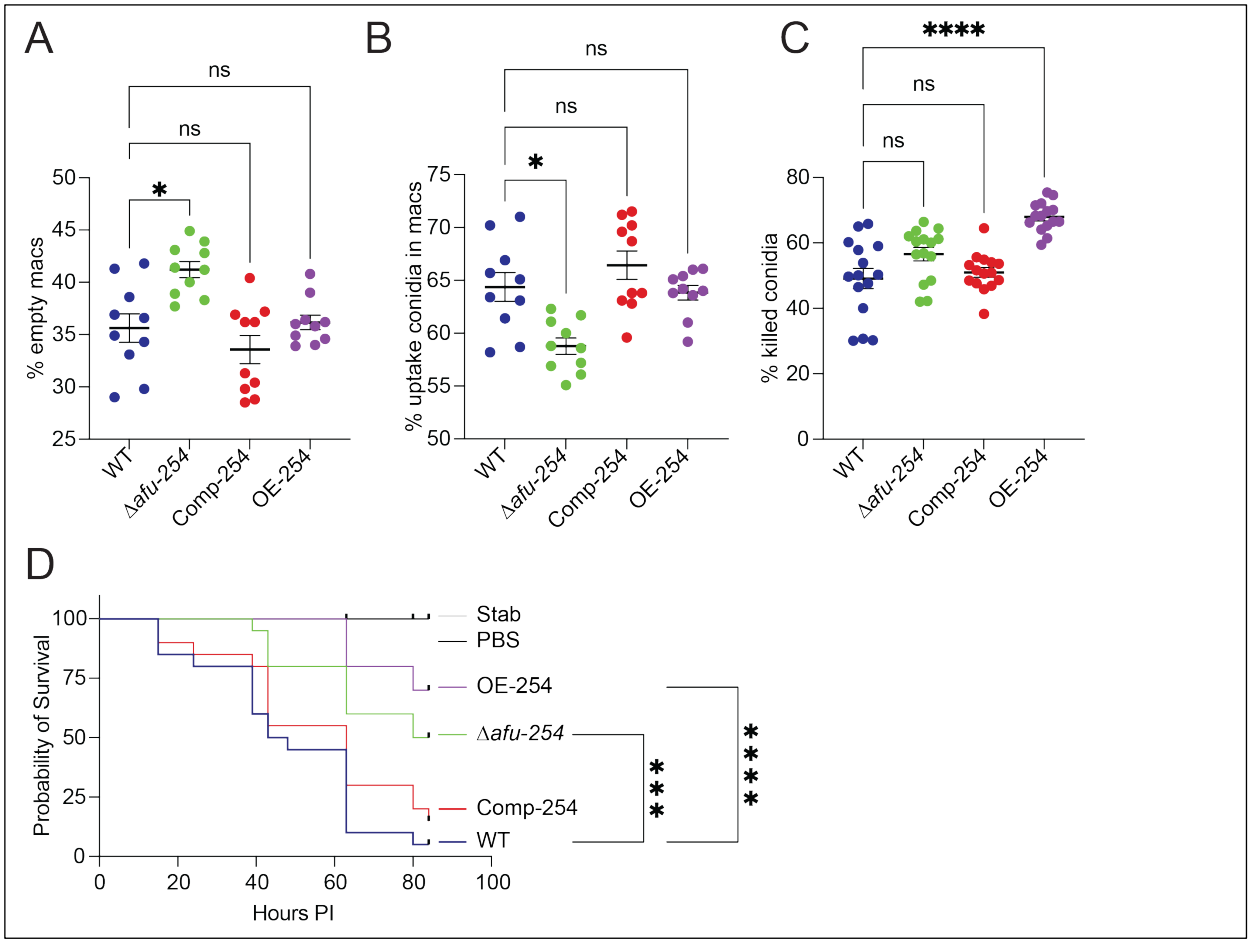

Figure 5: *afu-254* regulates fungal *ex vivo* killing and virulence in an invertebrate model of infection. BMDMs were incubated with conidia from the indicated strain (5:1 conidia to cell) that were biotinylated and stained with AF633 for 3 hrs. Cells were collected, and the percentage of live BMDMs (A) with (uptake) or (B) without (empty) conidia was determined by gating on AF633+ vs AF633- BMDMs using flow cytometry. The Δ*afu-254* strain showed less uptake by BMDMs. The points represent combined data from 2 experiments. (C) BMDMs were incubated with conidia from the indicated strains (5:1 conidia to cell) for 5 hrs. Cells were lysed, and CFUs were determined by serial dilution and plating. Results depict the percentage of killed conidia from three independent experiments compared to the starting inoculum. The OE-254 strain shows statistically increased killing by BMDMs, whereas the Δ*afu-254* strain trends towards increased killing, albeit not statistically significant. The Kruskal-Wallis test with Dunn's multiple comparisons was performed for statistical analyses. All error bars represent standard error. * $p<0.05$, **** $p<0.0001$. (D) *afu-254* is indispensable for virulence. *Galleria mellonella* larvae were infected with the 5 x

791 10^4 spores of the indicated strains of AF and monitored. The larvae exhibiting a lack of
792 movement upon physical stimuli were marked as dead (n=20 for all infected larvae, 10 for
793 controls). Survival was significantly different for the Δ*afu-254* strain and the OE-254 strain
794 compared to WT ($p<0.001$ and $p<0.0001$, respectively, log-rank test).

795

Figure S1:

Figure S1. RACE analysis to establish lncRNA *afu-254* boundaries. Chromatograms showing sequencing data for (A) 5' RACE or (B) 3' RACE. (C) Annotation depicting the major parts of sequencing results from 3' RACE showing the pJET vector sequence, primers used for making cDNA, 3' end and the splice site indicating the site of of 60bp intron (920 713 – 920 772).

Figure S2:

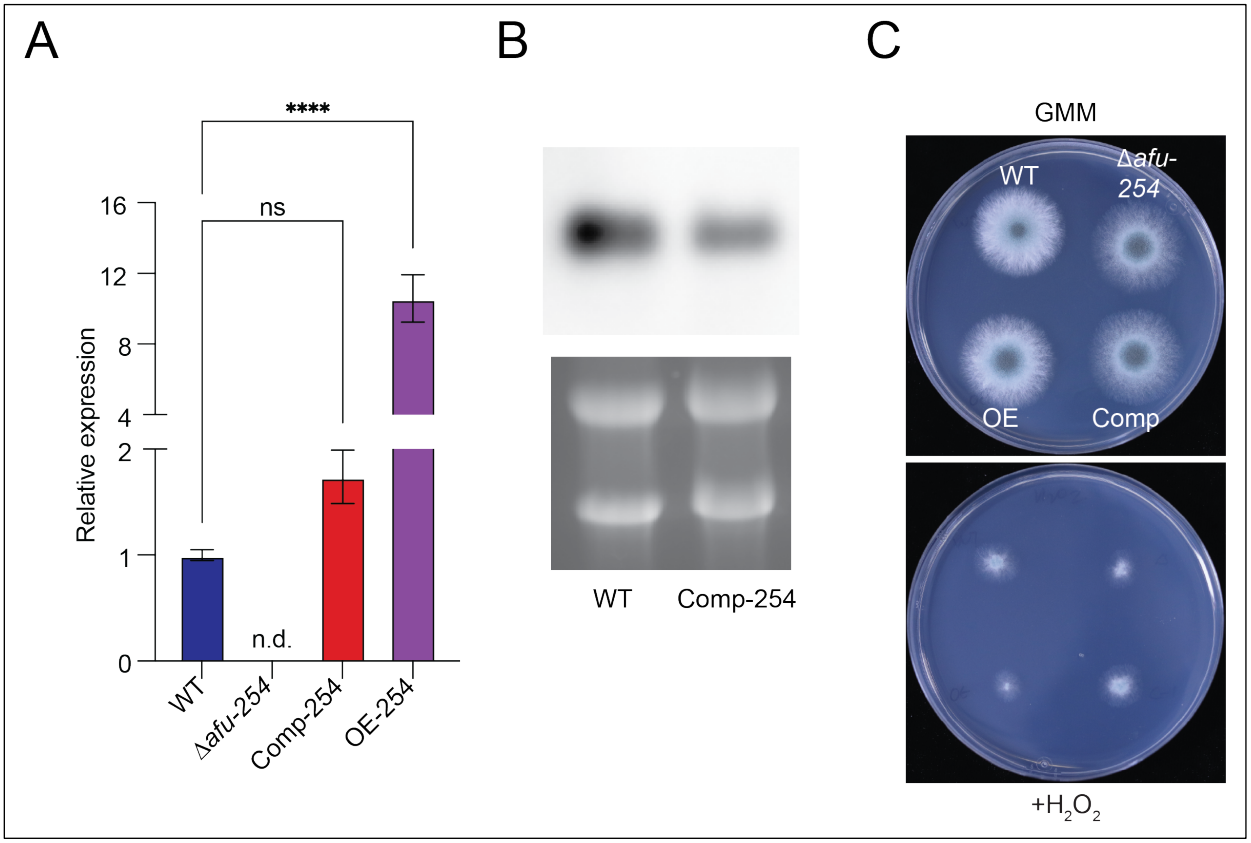

Figure S2. afu-254 is a non-essential ncRNA that plays a role in oxidative stress response. (A) qPCR analyses showing the relative expression levels in Comp-254 and OE-254 strains compared to WT. No transcript was detected in Δ*afu-254* strain. (B) Northern blot analysis to compare the RNA level in the WT and the Comp-254 strain. (C) Spot analysis showing a role of *afu-254* in oxidative stress response in the presence of 3mM H_2O_2.

Figure S3:

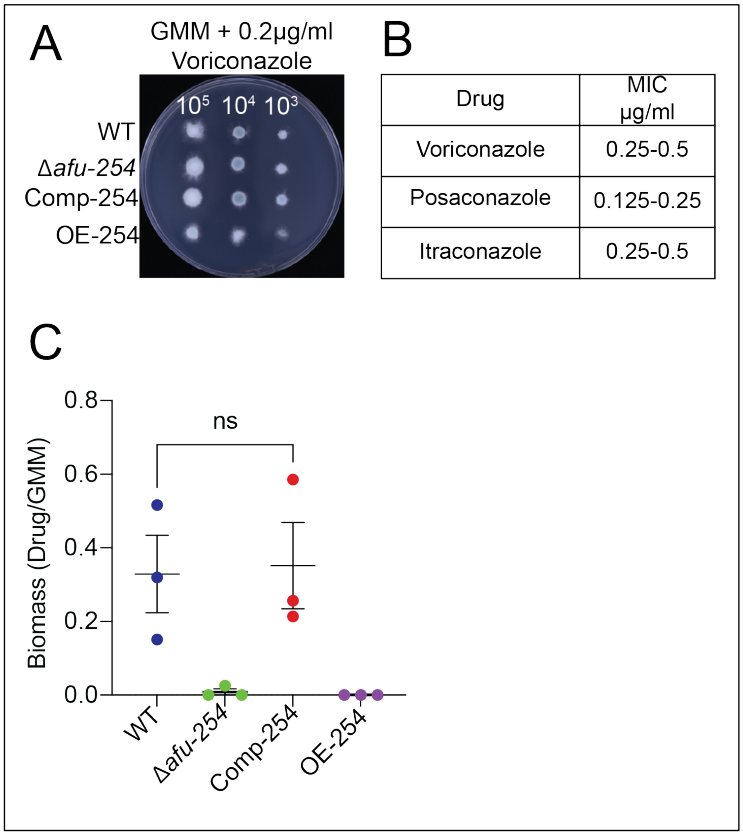

Drug	MIC µg/ml
Voriconazole	0.25-0.5
Posaconazole	0.125-0.25
Itraconazole	0.25-0.5

Fig S3. *afu-254* mediates fungal response to posaconazole and itraconazole but not voriconazole. (A). Spot assay (10^5-10^3) was done in the presence of 0.2µg/ml voriconazole, and plates were incubated at 37°C for 48 hours and photographed. (B) MIC levels of voriconazole, posaconazole and itraconazole are the same for all strains as tested via broth microdilution assay. (C) Fungal spores were inoculated in 50ml of media in a baffled flask and were grown at 37°C for 24 hours with constant shaking at 250rpm without or with 0.03µg/ml posaconazole. Fungal biomass was collected and represented as a ratio of dry weight between treated vs untreated samples.

867 Supplementary Table 1 – List of strains

Strain	Source
CEA10	Cramer Lab (Dartmouth)
CEA17	Cramer Lab (Dartmouth)
Δ*afu-254*	This study
Comp-254	This study
OE-254	This study

868

869

Table 2: List of primers

Primer Name	Sequence (5'→3')
SD284	ATGGACTCTGGTGGAGGTGG
SD366	CTGAGAGTGCCTTTCTGGTGGTC
SD78	GCAACGCTTCGTTCACCATCAAC
SD266	CGCATCAGTGCCTCCTCTCAGACATCCTATTATCACCCACGCTCTTACGC
SD267	TGTACGTTTGCATCTCAACTGACAGC
SD 218	GCCAGAGAAGATGTGGGCAATCTC
SD219	AGAGCATTGTTTGAGGCGACCGGTTAGCCCTGTTCACTGACGTAGTCATG
SD1	ACCGGTCGCCTCAAACAATGCTCT
SD2	GTCTGAGAGGAGGCACTGATGCG
SD222	CCAAGGCTGTGACCGAAGCTC
SD437	ACAACAGTCTTCGGCTAGACTCG
SD580	NNNNNNNNGGCGCGCCTACGTCAGTGAACAGGGCTACACG
SD581	NNNNNNGCGGCCGCACAACAGTCTTCGGCTAGACTCG
SD134	CGAAGGCTTGGGGCACCTG
SD103	GGGAAAAGAAAGAGAAAAGAAAAGAGCA
SD 468	TGCTCTTTTCTTTTCTCTTTCTTTTCCCTTTGTTACTCACCCAGAGGCC
SD202	NNNNNNGGCGCGCCCGCCAATAGCTTTGGGACGATGC
SD136	NNNNNNGGCGCGCCCGAGCTCCCAAATCTGTCCAGATC
SD323	NNNNNNGCGGCCGCGTCAGTGAACAGGGCTACACGC
SD 375	CCGCCGTGGTGGTGTCAAG
SD 376	GGCGTGTTCAGTGTAGGTGACG
SD201	CCCGAATTGGCATATCTCACGACG
SD188	CAACACTGACCTCTGCGTTTCG

Figure 1:

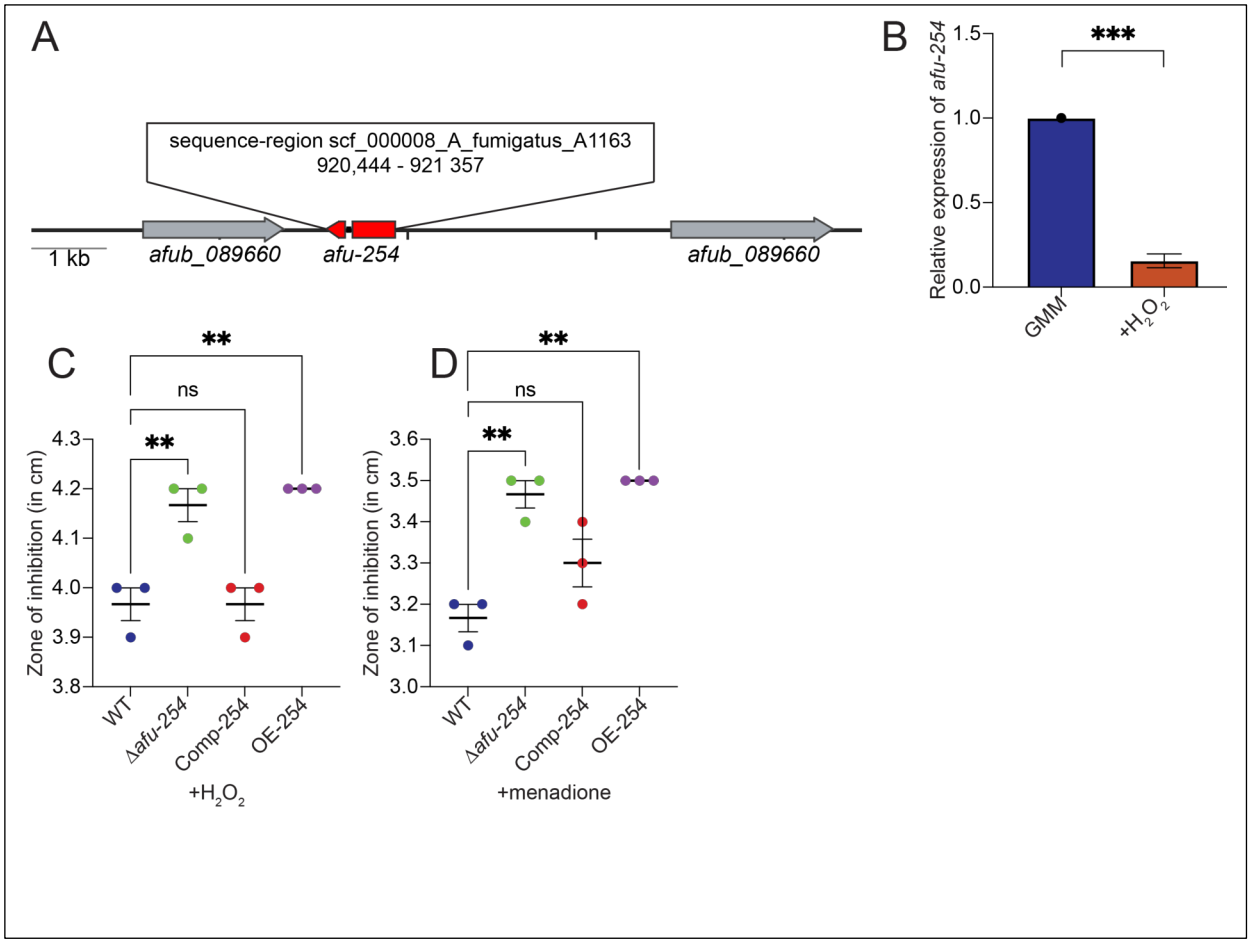

Figure 1. *afu-254* is an lncRNA that regulates fungal oxidative stress response. (A) 5' and 3' rapid amplification of cDNA ends confirmed the boundary of *afu-254* in the genome as indicated. (B) qPCR analysis showing the relative levels of *afu-254* in the presence of oxidative stress compared to GMM. Fungal strains were inoculated in top agar. After solidification, a core was cut in the center using a sterile pipette tip, and 100µl of either (C) 5mM H_2O_2 or (D) 2mM menadione was added. The zone of inhibition was measured after 36 hours and represented. ** $p<0.01$, *** $p<0.001$, ns – not significant

Figure 2:

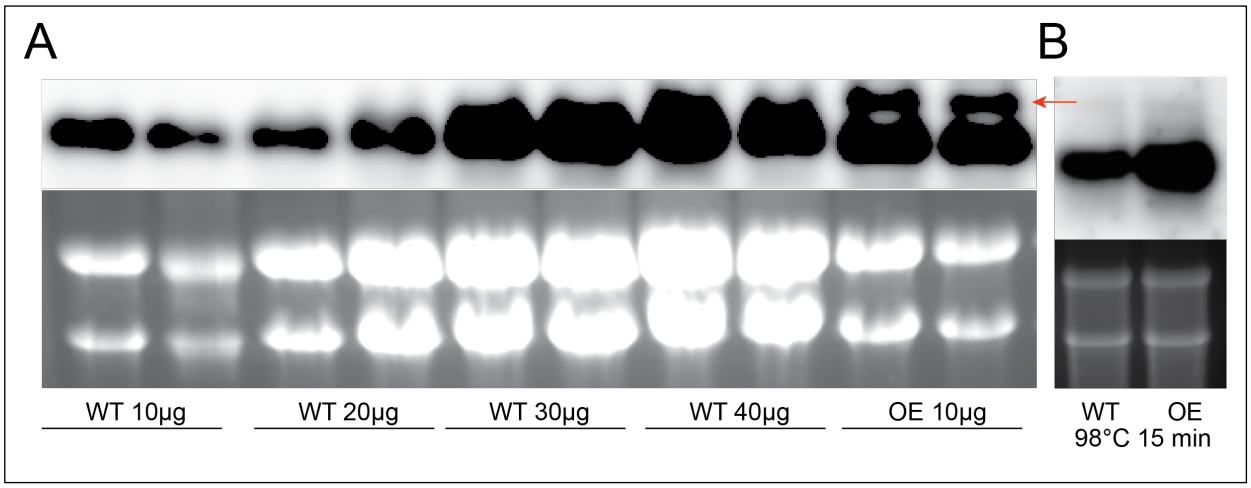

Figure 2. OE-254 constitutes an anamorph. (A) WT and OE-254 RNA were loaded in a denaturing formaldehyde gel at the indicated concentration. The samples were heated at 65°C for 5 min before loading. The OE-254 strain shows the presence of a higher molecular weight band (red arrow). (B) The samples were heated at 98°C for 15 mins, leading to loss of the higher molecular weight band.

Figure 3:

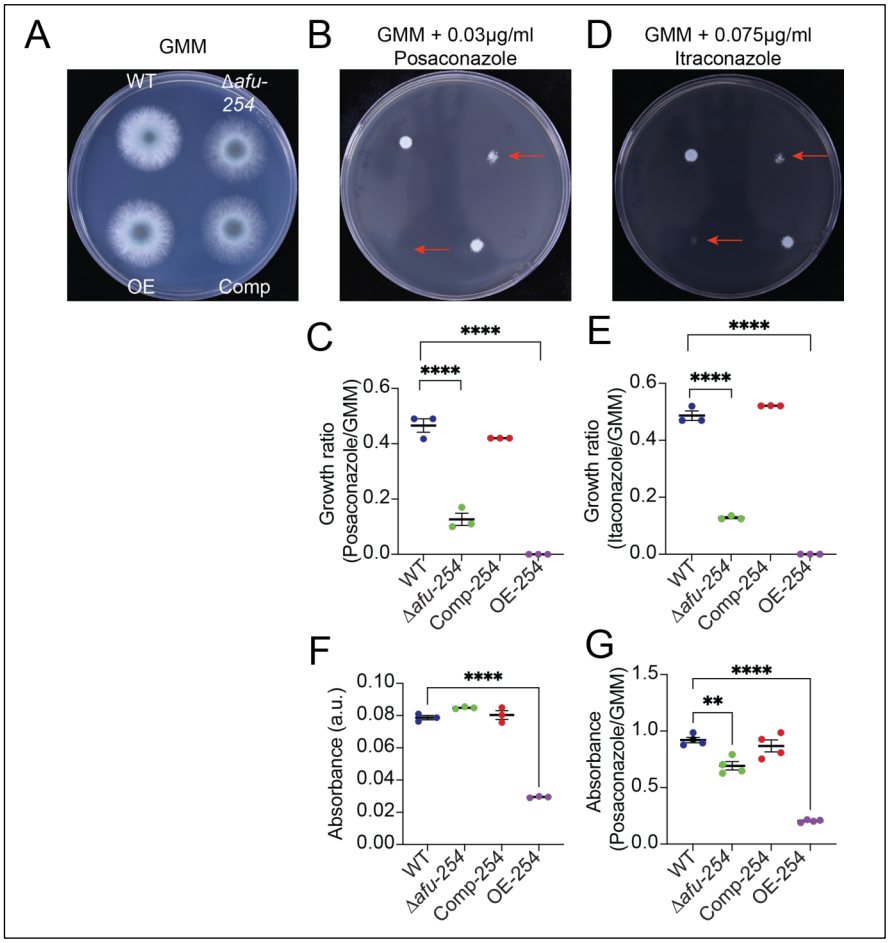

Figure 3. *afu-254* plays a role in fungal response to posaconazole and itraconazole on solid medium and surface attached cultures. Fungal strains were spot inoculated (10^4 spores) in (A) absence of drug or presence of (B and C) posaconazole or (D and E) Itraconazole. Both Δ*afu-254* and OE-254 show increased susceptibility to long tailed azoles. (D and E) Quantitative measurements of fungal growth after 48 hours are represented as a ratio of fungal growth in the presence and absence of the indicated drug. (F) *afu-254* plays a role in fungal surface attachment. Fungal strains were allowed to adhere to the abiotic surface for 12 hours. The surface attached cultures were then (F) left untreated (GMM), treated with posaconazole for 8 hours (GMM + 0.2µg/ml posaconazole), washed and stained with crystal violet. (F) Values represent the absorbance of untreated samples. The OE-254 strain shows decreased surface attachment. (G) Values represent the ratio between absorbance measured after azole treatment and fungal attachment before treatment at the 12-hour time point. a.u. – arbitrary units. **** $p<0.0001$, One-way ANOVA.

Figure 4:

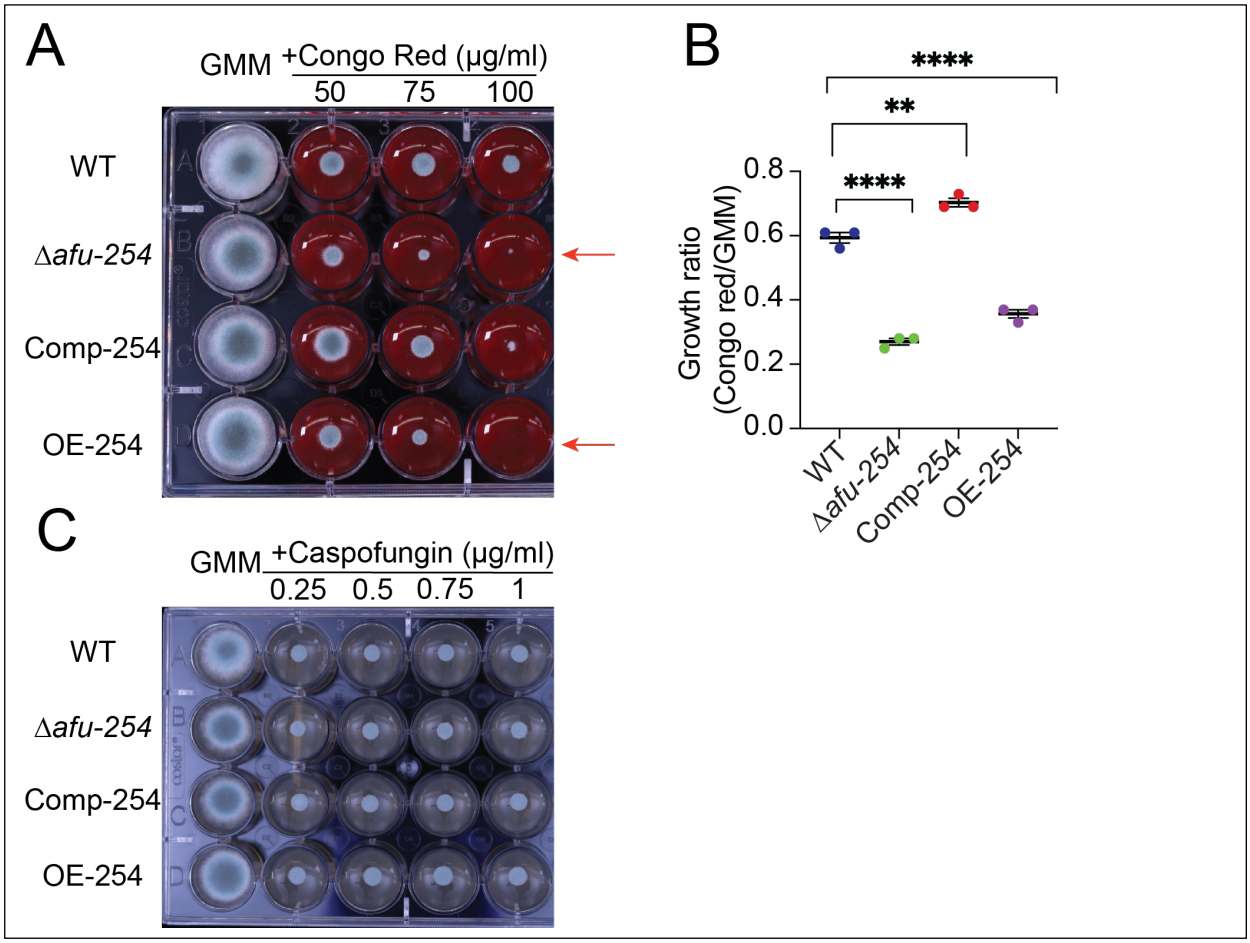

Figure 4. *afu-254* mediates fungal cell wall response to Congo red but not to Caspofungin. Fungal strains were spot inoculated (10^4 spores) in a 24 well plate in the absence or presence of indicated concentrations of (A) Congo red or (C). Caspofungin. Both Δ*afu-254* and OE-254 strains are susceptible to Congo red (red arrows) but not to Caspofungin. (B) Quantitative analysis of fungal growth is represented as a ratio between growth in the presence of CR and the absence of CR. ** $p<0.01$, **** $p<0.0001$.

Figure 5

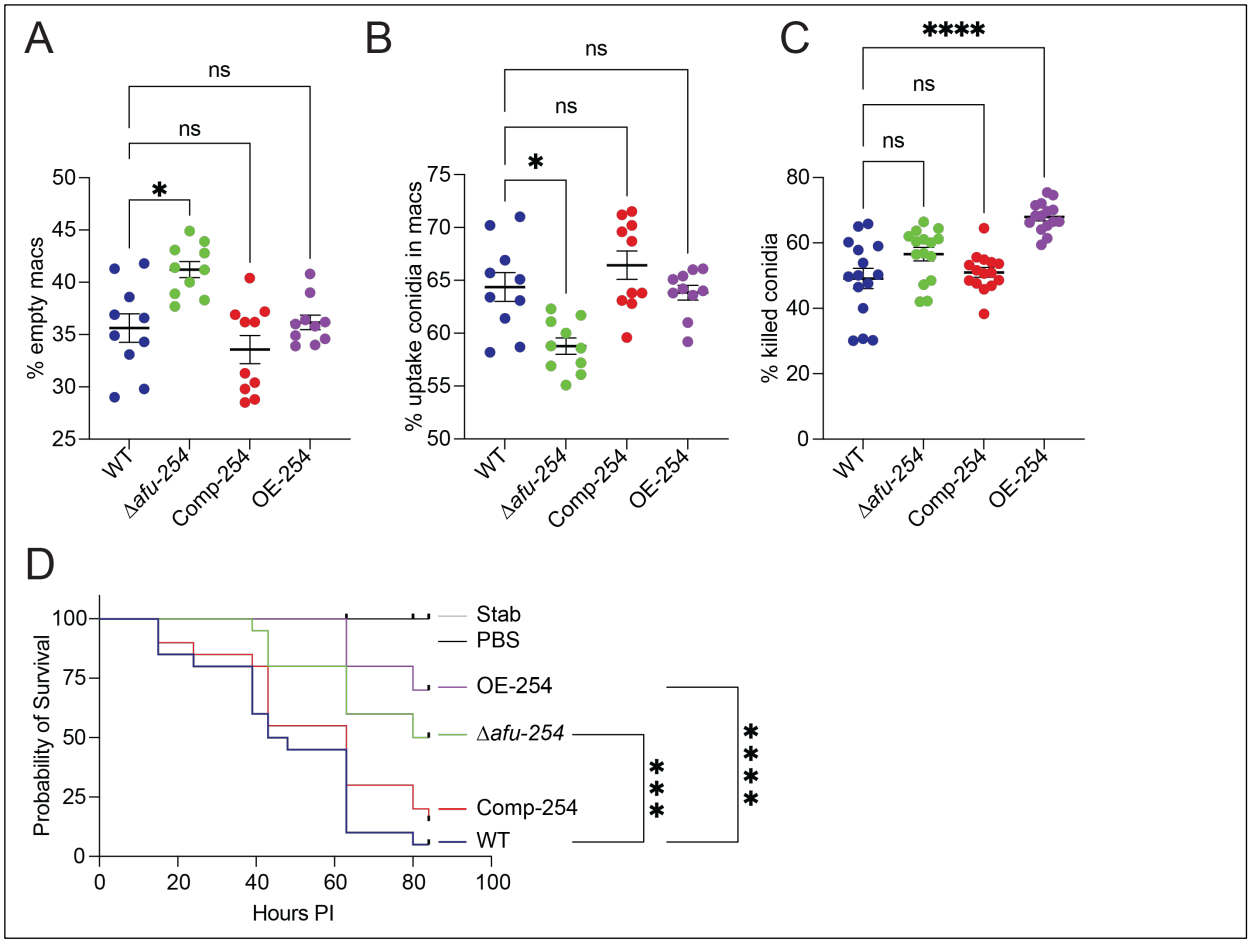

Figure 5: *afu-254* regulates fungal *ex vivo* killing and virulence in an invertebrate model of infection. BMDMs were incubated with conidia from the indicated strain (5:1 conidia to cell) that were biotinylated and stained with AF633 for 3 hrs. Cells were collected, and the percentage of live BMDMs (A) with (uptake) or (B) without (empty) conidia was determined by gating on AF633+ vs AF633- BMDMs using flow cytometry. The Δ*afu-254* strain showed less uptake by BMDMs. The points represent combined data from two experiments. (C) BMDMs were incubated with conidia from the indicated strains (5:1 conidia to cell) for 5 hrs. Cells were lysed, and CFUs were determined by serial dilution and plating. Results depict the percentage of killed conidia from three independent experiments compared to the starting inoculum. The OE-254 strain shows statistically increased killing by BMDMs, whereas the Δ*afu-254* strain trends towards increased killing, albeit not statistically significant. The Kruskal-Wallis test with Dunn's multiple comparisons was performed for statistical analyses. All error bars represent standard error. * $p<0.05$, **** $p<0.0001$. (D) *afu-254* is indispensable for virulence. *Galleria mellonella* larvae were infected with the 5 x

10^4 spores of the indicated strains of AF and monitored. The larvae exhibiting a lack of movement upon physical stimuli were marked as dead (n=20 for all infected larvae, 10 for controls). Survival was significantly different for the Δ*afu-254* strain and the OE-254 strain compared to WT ($p<0.001$ and $p<0.0001$, respectively, log-rank test).